JMEPEG (2020) 29:7408–7419
https://doi.org/10.1007/s11665-020-05181-2

1059-9495/$19.00

Experimental Investigation on the Effects of Core/Facing Interface Performance on the Low-Velocity Impact Behavior of Honeycomb Sandwich Panels

Ahmet Meram and Mehmet Emin Çetin

(Submitted May 25, 2020; in revised form August 26, 2020; accepted September 8, 2020; published online October 15, 2020)

This paper gives an important contribution by investigating the effectiveness of core/facing interface performance of aluminum honeycomb sandwich panels under low-velocity impact energy. Low-velocity drop tests were conducted on five different panels under 50, 75, and 100 J impact energies (loads). The following procedure is followed to evaluate the impact response of panels: the force–time histories are acquired; the numerical integration method is applied, and force–displacement histories are obtained; and then the damage mechanism and theoretical energy balance modeling are used to analyze the effectiveness of core/facing interface performance on the impact behavior of the panels. Scanning electron microscopy is used to examine the microstructural and the morphology of the core/face sheet interface of the aluminum honeycomb sandwich panels. The effects of voids, interface, and cohesive cracks on the impact behavior of the panels are analyzed. Energy balance modeling proved that energy absorbed in the bending and shear deflections increased as the resistance at the core/facing interface is increased. In addition, changing the initial impact energy from 50 to 100 J produced more than 120% increase in the effectiveness of the panels in terms of energy absorbed in shear and bending deformations.

Keywords core/facing interface, energy balance model, failure mechanism, honeycomb sandwich panel

1. Introduction

Honeycomb sandwich panel is a three-layer structure panel, consisting of a top and bottom skin sheet with a honeycomb core at the middle, which are bonded together by interface adhesive layer. These structures are widely used in aerospace, military, automotive, railway, and marine industries due to its lightweight and high stiffness (Ref 1-7). During its entire life, these structures are exposed to impact stresses due to various factors. The localized impact load can cause damage to sandwich panels, which results in reduction of load-carrying capacity of the sandwich panel and reduced performance. Because of this fact, investigation on the impact response of the sandwich panels has been receiving much attention from many researchers (Ref 8-11). Generally, theoretical, numerical, and experimental approaches are used to investigate the low-velocity impact response of the sandwich structures (Ref 12-15). For instance, Foo et al. (Ref 16) numerically investigated the effect of various geometric parameters on the low-velocity impact response of aluminum honeycomb sandwich panels. Zhang (Ref 17) experimentally investigated the energy absorption capacity of aluminum sandwich panels under low-velocity impact loading using a spherical projectile. Moreover, there are some reported studies related to deflection, energy absorption, and contact force of the impactor on the low-velocity impact behavior of honeycomb sandwich panels (Ref 18-20). Wang (Ref 21) conducted impact tests on sandwich panels with various cores and proved that polypropylene honeycomb core is the best choice with minimum deformation on the bottom skin sheet. Apart from the above, the effects of other parameters such as material (Ref 22-26), impactor shape (Ref 27), geometric configuration (Ref 28-31), face sheet thickness (Ref 32), foam-filled core (Ref 33), and failure mechanism (Ref 34-37) are also investigated by researchers.

In honeycomb sandwich panels, the adhesive joins the edges of a thin flexible cell wall with a stiff sheet (Ref 38). The adhesive spreads the loads between layers, which increases the stiffness and strength of the sandwich panel structure (Ref 39). Although the strong joint between the core material and the skin sheets is a vital element in sandwich panels, only fewer studies (Ref 40-43) considered the effect of adhesive on the impact response of honeycomb structures. For example, Zhang et al. (Ref 41) simulated the impact behavior of honeycomb sandwich panels with adhesive layer and without adhesive (perfect bonding) and found that the results of model with adhesive are better than the model without adhesive. Zarei Mahmoudabadi (Ref 42) proved that the existence of adhesive layer between top skin and honeycomb core increased the specific energy by 12%. Liu et al. (Ref 43) experimentally investigated the effect of adhesive surface thickness on critical buckling load of honeycomb sandwich panels. All previous studies have mainly focused on the comparison of impact behavior of sandwich panels with and without bonded core/-face, neglecting the core/facing interface performance. Motivated by this fact, this literature experimentally investigates the influence of core/facing interface performance on the various parameters such as failure mechanism, initial threshold force, peak force, structural stiffness, shear, bending, and contact

Ahmet Meram, Department of Mechatronics Engineering, KTO Karatay University, Konya, Turkey; and **Mehmet Emin Çetin**, Department of Astronautical Engineering, Necmettin Erbakan University, Konya, Turkey. Contact e-mail: mecetin@erbakan.edu.tr.

energy absorption of honeycomb sandwich panels under three different initial impact energies. Moreover, microstructure of the face/core interfaces is also analyzed utilizing a SEM images.

2. Materials and Methods

Five different aluminum honeycomb sandwich panels (specimens) are used for impact tests in our experiment. The dimensions of specimens are provided with uniform geometric specifications shown in Fig. 1. The dimensions of honeycomb core are 100 × 100 × 20 mm. The hexagonal core is fabricated from Al 3003-H19 foil sheet with 0.05 mm thickness and 10.4 mm cell size as shown in Fig. 1. Five different bonding elements are used on the core/facing interface. Table 1 shows the interface resistances of the bonders in the order of increasing resistance value.

A drop weight test machine is used to conduct low-velocity impact tests as shown in Fig. 2. An appropriate fixture is used to hold the specimen. This fixture provides symmetric boundary condition, and so it eliminates the specimen's size effect on the experimental results. The test machine consists of many components such as dropping mass, guiding rails, load sensor, projectile with semi-spherical nose with diameter of 24 mm with data acquisition and processing system. The data acquisition system uses a National Instruments Signal Express data acquisition software and a post processor. The dropping mass is released from different heights to obtain axial impulsive loading. Table 2 lists the various parameters such as height, dropping mass, corresponding initial velocity, and impact energy. The experiments are carried out with an impactor mass of 20 kg and with 50, 75, and 100 J initial impact energies according to ASTM D7136 standards energies. Load–time histories are measured by a PCB Quartz ICP force sensor (200B04). The force sensor with frequency range 0.0003–75,000 Hz is specifically designed for impact force measurements. During the experimental study, each test condition is repeated three times to achieve the reliability of experimental results. It is observed that the deviation between the results can be neglected. Newton's second law of motion and numerical integration method are applied to obtain the acceleration, velocity, and displacement of the projectile according to the ASTM D7136 standard.

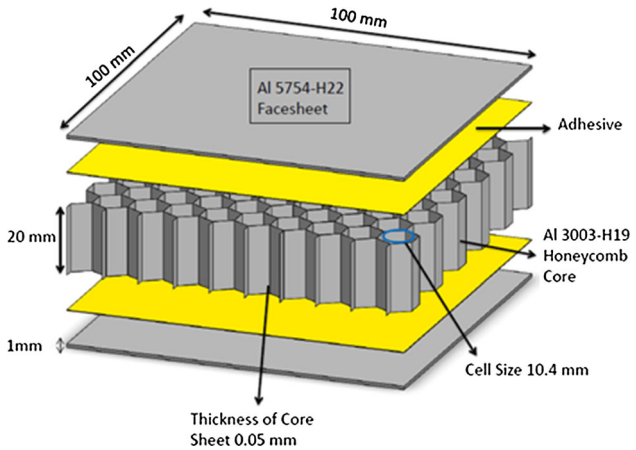

Fig. 1 Schematic view of honeycomb sandwich panel specimen with geometric and material specifications

3. Results and Discussion

This section presents the results of low-velocity impact tests of panels with five various adhesives under three different initial impact energies 50, 75, and 100 J, and results are analyzed and discussed.

3.1 Failure Mechanism

Figure 3 shows the top and section views of specimens after the impact tests with 50, 75, and 100 J initial impact energies. Generally, indentation failure is the most effective failure mode in impact loading (Ref 44). The analysis of specimens after impact tests proves that the projectile penetrates the top skin sheets of all sandwich panels and permanent indentation can be seen right below the projectile. Moreover, wrinkling and local plastic deformation appear on top surface. Global bending occurs on the bottom skin sheet. The honeycomb core is buckled, and progressive crushing is observed. When the initial impact energy is increased, the wrinkling on top skin, bending in bottom skin, and densification in honeycomb core are increased. The typical cross section of the impacted specimen is shown in Fig. 4. Debonding at the core/facing interface has occurred in specimens fabricated using bonder with Adh-1 and Adh-3 having 11.2 and 14.3 MPa interface resistance, respectively. Because of debonding, the specimen loses the structural integrity and the stiffness of the structure is decreased. It is noted that when the initial impact energy is increased, the debonding started to occur in large area of core/skin interface. So, the impact damage resistance of the sandwich panels can be improved by using high strength adhesives. The bonding between the top skin and honeycomb core transmits shear resistance of the honeycomb to the deformed region surrounding the projectile. This infers that debonding area in sandwich panel is decreased by increasing the resistance of the bonder. The debonding failure is not observed in specimens bonded using Adh-4 and Adh-5 bonders having 16.2 MPa and 17.1 MPa, respectively.

The microstructural and the morphology of core/face sheet interface of the aluminum honeycomb sandwich panels are analyzed using scanning electron microscopy (SEM) (Hitachi-SU 1510). SEM images of the adhesive core/face joints are photographed at 15 and 20 kV accelerating voltages for achieving the low and medium–high (100–1500×) magnifications. The test specimens after the impact tests under the impact energy 75 J are prepared for microstructural characterization. The SEM images of impact damage area of panels bonded with five different adhesives are given in Fig. 5(a), (b), (c), (d), and (e). The images reveal the reason of the improvement of the impact behavior of the panels with the increase in interface resistance. In addition, they explicitly explain the relationship between adhesive interface resistance and failure mechanisms. Interfacial areas of specimen with Adh-1in in Fig. 5(a) display severe interface and cohesive cracks, separation in adhesive fillets, and greater number of large voids. The presence of these types of defects results in the large deflections of the sheets leading to failures. It is concluded that these defects play an

Table 1 The core/facing interface resistance

No.	Specimen index	Adhesive commercial name	Density, kg/L	Interface resistance, MPa
1	Adh-1	Denlax	1.35	11.2 ± 0.3
2	Adh-2	Bostik	1.57	12.1 ± 0.2
3	Adh-3	Fabro	1.2	14.3 ± 0.4
4	Adh-4	Sege	1.47	16.2 ± 0.2
5	Adh-5	Klb75	1.35	17.1 ± 0.3

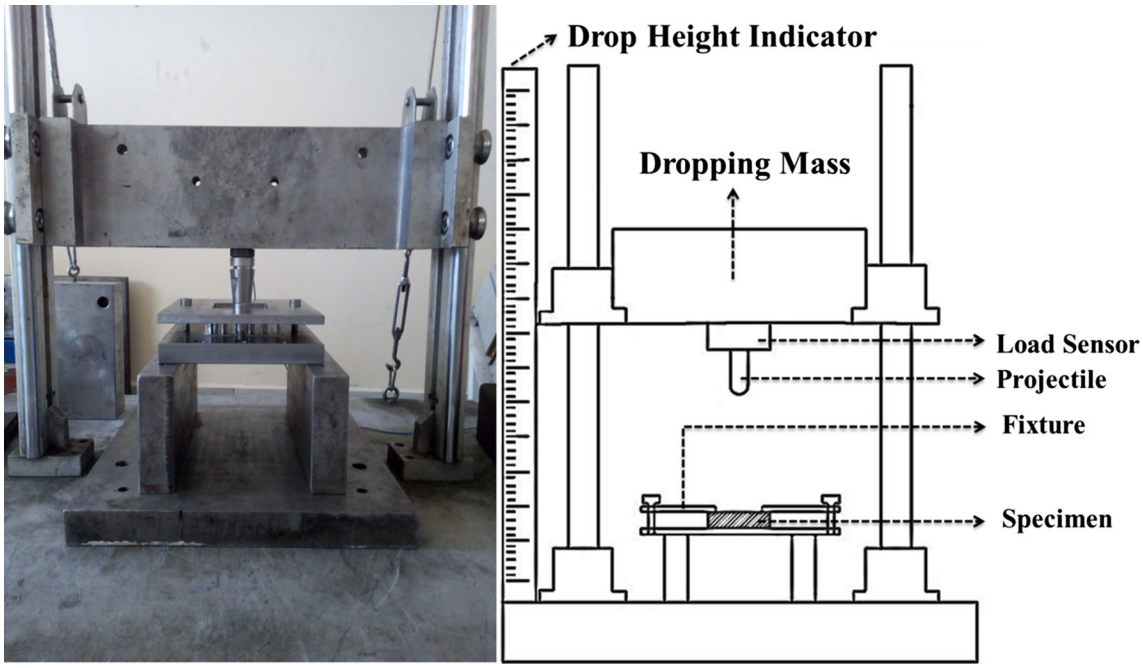

Fig. 2 Low-velocity drop test setup and schematic description

Table 2 The initial condition and mass of striker for three impact energies

Mass, kg	Drop height, mm	Impact velocity, m/s	Impact energy, J
20	255	2.24	50
20	382	2.74	75
20	510	3.16	100

important role in the impact failure of aluminum sandwich structures.

When the interface resistance value is increased, the voids and interface and cohesive cracks decreased as shown in Fig. 5(a), (b), and (c). Large increase in interface resistance reduces microdamages substantially, thus improving the impact performance of sandwich panels. But in specimen Adh-3, microcracks in transverse direction are observed as shown in Fig. 5(c), and it is not observed in others. Since the adhesives with high interface resistance values have improved adhesion and cohesion efficiency of the face/core bonding, hence there are no microcracks. Careful observation of damage area in specimen Adh-4 shows that the adhesive contains only small and less voids. Contrarily, voids, transverse adhesive cracks, and interface cracks are not formed in specimen adh-5. This shows that better adhesion between core and face has occurred in specimen Adh-5 compared to Adh-4. Lack of the voids and cracks inhibits failure formation and propagation. Finally, fractography shows great differences in core/face interface microstructures of specimens, which demonstrated that bonding has different amplification effects on impact failure behavior.

3.2 Load–Time and Load–Deflection Histories

The impact load curves help to quantify structural responses and demonstrate the failure mechanisms under impact loads. Figure 6, 7, and 8 exhibit load–time and load–defection histories for each experiment. Typically, all the curves consist of an elastic linear stage, the plateau stage, and the densification stage. The first stage of curve represents the occurrence of

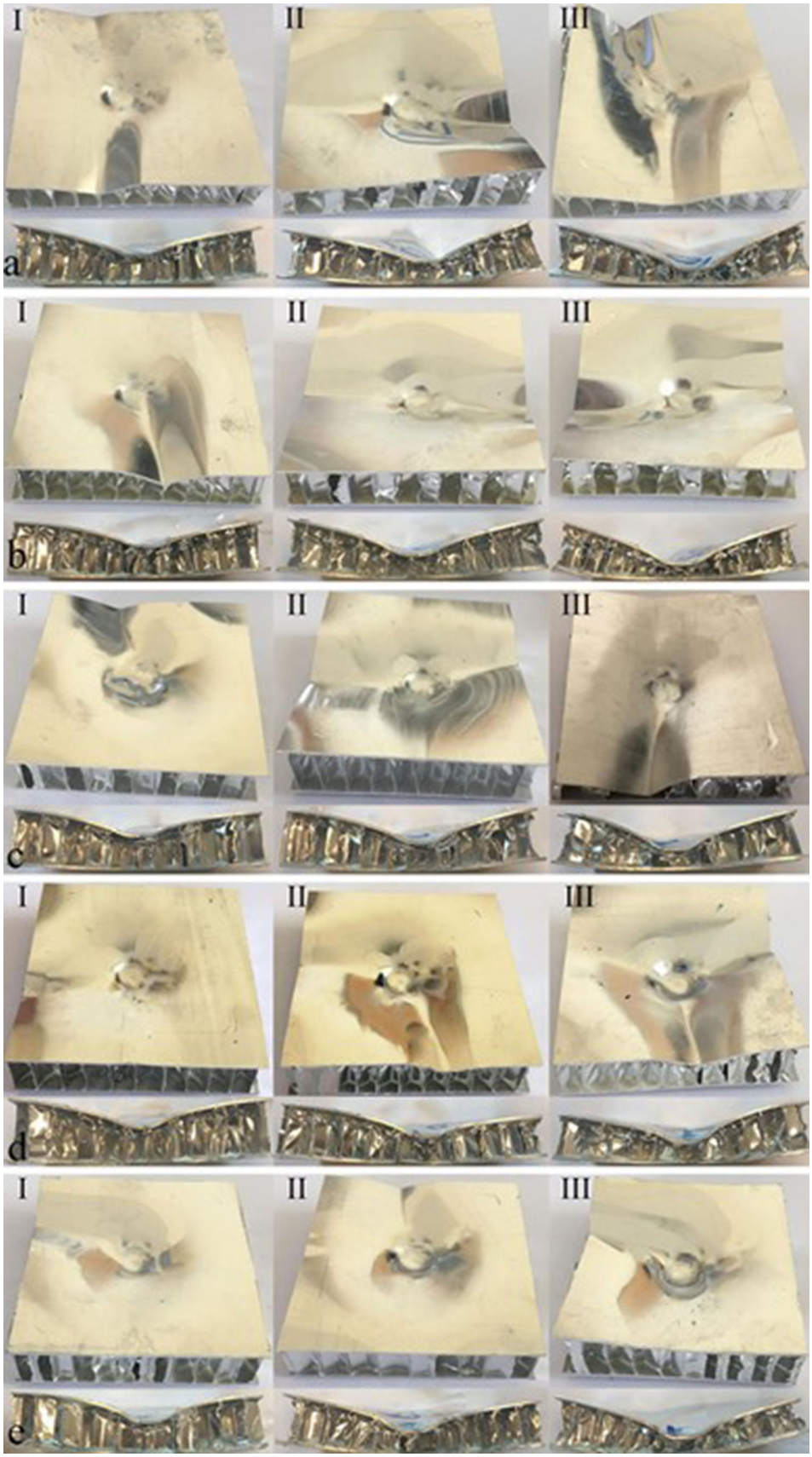

Fig. 3 The top and cross-sectional views of damaged specimens bonded with adhesives: (a) Adh-1, (b) Adh-2, (c) Adh-3, (d) Adh-4, (e) Adh-5 with initial impact energies (I) 50, (II) 75, and (III) 100 J, respectively

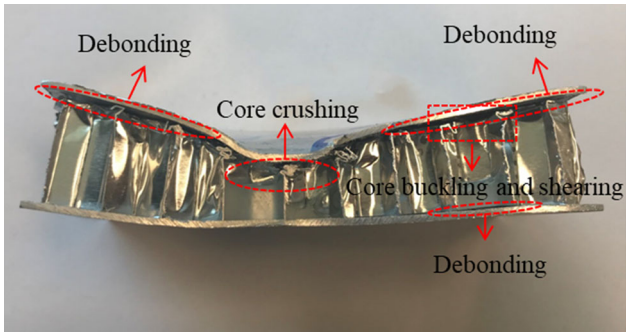

Fig. 4 The typical cross section of the impacted specimen with failure mechanisms

global bending after the projectile impact of the sandwich panel. The slope of the linear region represents the stiffness of the sandwich panel. As illustrated in Fig. 6, 7, and 8, the increase in the interface resistance leads to increase in the slope of the load–deflection curves. Due to the plastic deformation in top skin sheet, a sudden drop in contact load follows the linear regime. Then, local buckling and progressive crushing occur on the honeycomb core. When there is continuous compression (crushing) of the panels, the load–deflection curves continue to display in plateau stage. After that, the impact force reaches up the peak load due to densification in honeycomb core. Finally, the projectile loses its kinetic energy and the impact force drops. The analysis of load–time and load–deflection curves proves that an increase in the interface resistance improves the initial impact energy and the load-carrying capacity of the sandwich panels. Moreover, the increase of interface resistance increases the contact duration and reduces the deflection of sandwich panels.

The peak force values and error bars of specimens with different initial impact energies are plotted in Fig. 9. It can be observed that the peak force of sandwich panel bonded with Adh-5 is about 50% higher than the one bonded with Adh-1 under 50 J impact energy category. It is observed that by increasing the impact velocity the effectiveness of interface resistance on the peak force increases.

3.3 Initial Threshold Force

The initial threshold force values are considered to analyze the relation between the interface resistance and the impact response of sandwich panels in elastic stage. The initial threshold force shows physically the end of the linear-elastic response of the sandwich panel (Ref 40). After this stage, permanent damage of top skin sheet, the core/facing interface layer damage, and crushing of honeycomb core occur. Initial threshold force values are determined from the load–deflection curves. It can be seen from Fig. 10 that the impact force increases linearly with deflection in the first stage until the force reaches the initial threshold force. Then, the impact force increases slightly in nonlinear manner to reach the maximum force. Finally, the impact force decreases slightly with deflection. Figure 11 exhibits the average initial threshold force values and error bars under different initial impact energies. It is observed that increasing the resistance of interface increases the initial threshold force. Specimen Adh-5 with high interface resistance produces an initial threshold force approximately 50% higher than that of the specimen Adh-1.

3.4 Structural Stiffness

The slope of linear section in initial stage of load–deflection curve represents structural stiffness (Ref 40). The structural stiffness values of specimens under various initial impact velocities are plotted in Fig. 12. It is observed that high strength adhesive (Adh-5) creates structural stiffness about 26% higher than the low strength adhesive (Adh-1). These results are similar to and agree with earlier research work (Ref 40) conducted on specimens with and without adhesive. In sandwich panels, the core/facing interface layer contributes significantly in transferring of load from skin sheet to the honeycomb core. The obtained high value of structural stiffness proves the effectiveness of high interface resistance in transforming load from skin sheet to the core.

3.5 Energy Balance Model

The honeycomb sandwich panels absorb and dissipate the energy by means of various formations occurred in the panels such as bending of structure, permanent damage of top skin sheet, and honeycomb core crushing. Small deformation in the bottom skin sheet shows that there is only negligible energy absorption by the bottom sheet. In the first stage, the global bending occurs on the structure due to impact. Then, the energy is absorbed by the skin resulting in initiation of damage of top skin. Finally, the energy is absorbed leading to the crushing of honeycomb core.

In low-velocity impact analysis of sandwich structures, contact laws with spring-mass model are generally applied by researchers. The sandwich structure is modeled as a combination of a linear spring and a nonlinear spring in spring-mass model (Ref 34, 45). The linear and nonlinear springs represent the global deflection and the local indentions effects, respectively. The global deflection occurs in specimens due to the shear and the bending of the entire sandwich panel, whereas the local deflection occurs as a result of indentation of the top sheet and core crushing. Under the low-velocity impacts, since the impact damage is restricted around the impactor, the local and global deflection of the sandwich panel can be computed separately. To investigate the relationship between the core/facing interface performance and the low-velocity impact response of honeycomb sandwich panels, a theoretical approach according to the energy balance model has been applied. The energy balance model had been employed by researchers (Ref 34, 46) to predict the impact response of sandwich panels with honeycomb and foam cores with 50-200 kg/m^3 density. The density of the honeycomb cores tested in this study is 160 kg/m^3; thus, this model can predict the energy absorption of the investigated honeycomb sandwiches with adequate accuracy. Based on the energy balance model, total initial kinetic energy of the impactor absorbed by the sandwich panel due to the shear, bending, and contact effects can be presented mathematically by the following equation.

$$\frac{1}{2}mv^2 = E_s + E_b + E_c = \frac{1}{2K_{sb}}F_i^2 + E_c \qquad \text{(Eq 1)}$$

where E_s, E_b, and E_c are energies which absorbed in shear, bending, and contact processes, respectively. Forasmuch as the shear and bending effects are appeared on the linear portion of the force–deflection curves, to compute the energy absorbed in the shear and bending, the linear stiffness (K_{bs}) and initial threshold force (F_i) values are used in Eq 2.

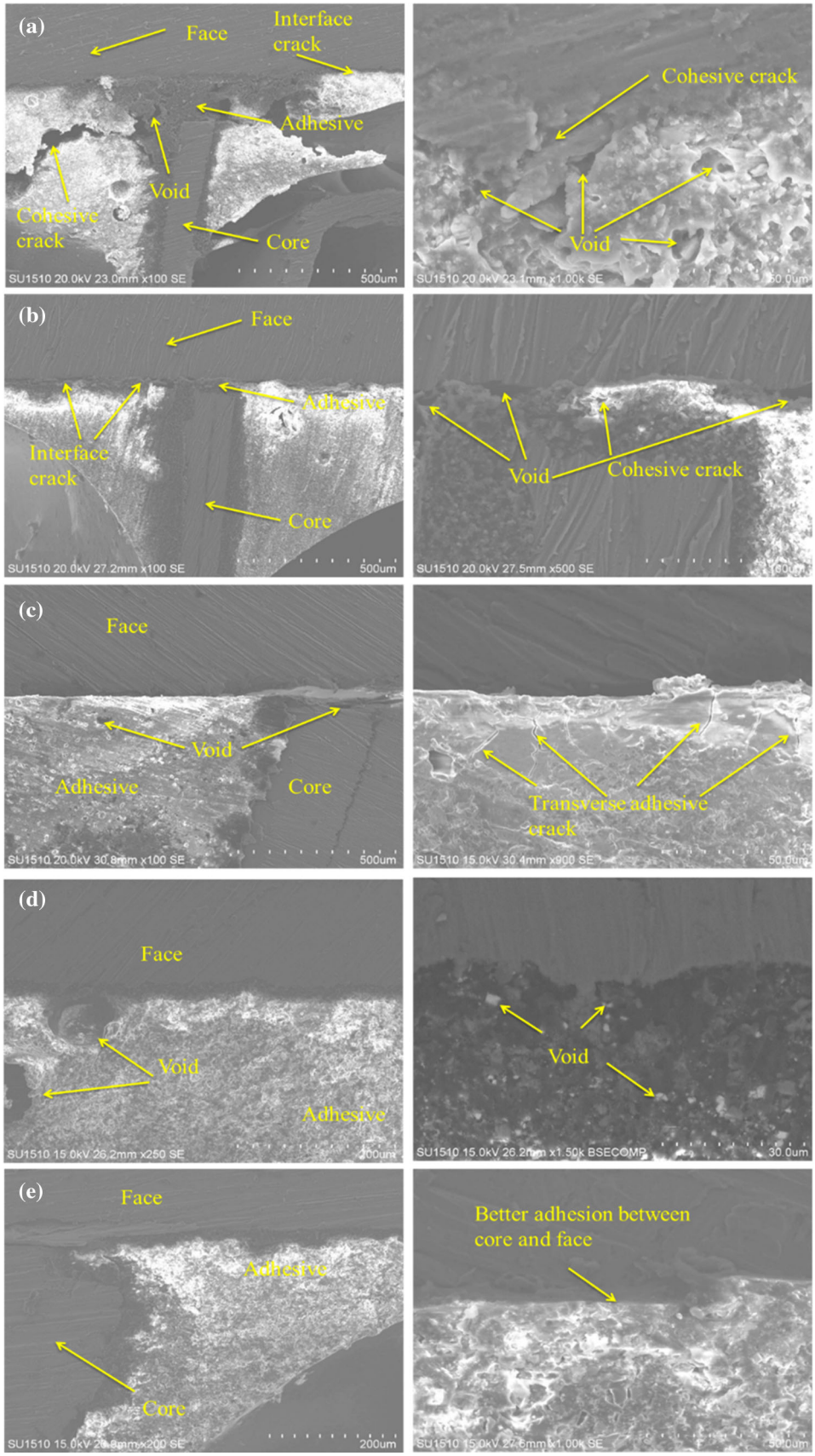

Fig. 5 SEM images of the damage area of core/face interface in sandwich panel tested at 75 J impact energy (a) Adh-1, (b) Adh-2, (c) Adh-3, (d) Adh-4, and (e) Adh-5

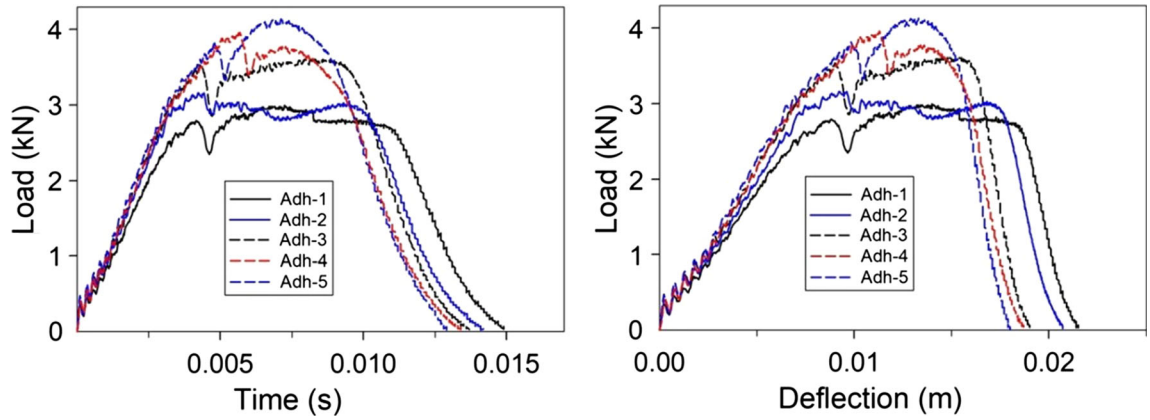

Fig. 6 Load–time and load–deflection histories for 50 J initial impact energies

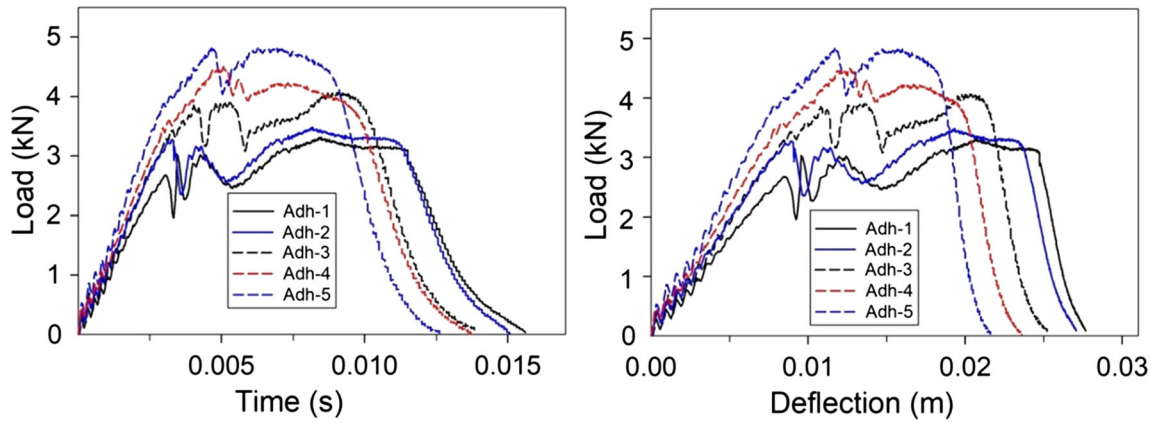

Fig. 7 Load–time and load–deflection histories for 75 J initial impact energies

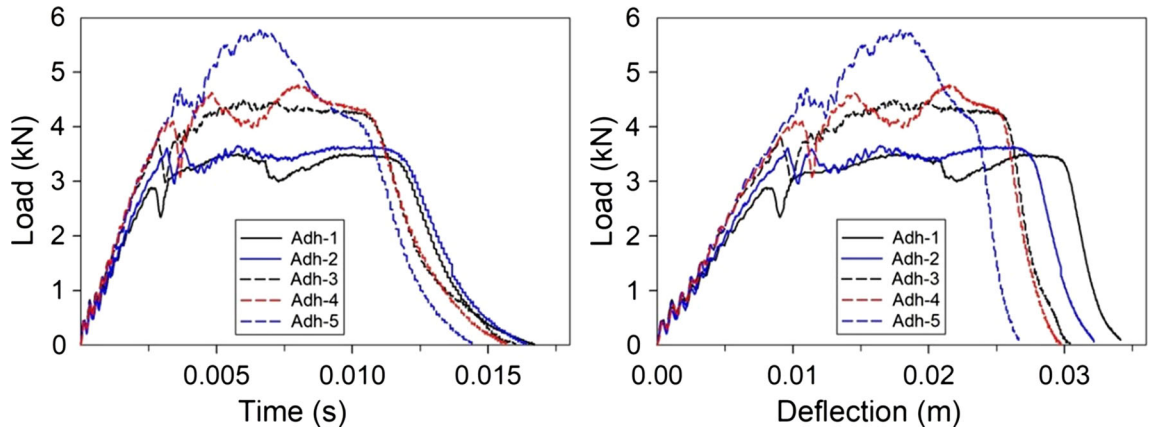

Fig. 8 Load–time and load–deflection histories for 100 J initial impact energies

$$E_{sb} = E_s + E_b = \frac{1}{2K_{sb}} F_i^2 \qquad \text{(Eq 2)}$$

The absorbed energy due to the contact effects is obtained (top sheet indentation and core crushing), subtracting the E_{sb} values from the total absorbed energy. The E_{sb} and E_c values for each specimen are plotted in Fig. 13 and 14 in three initial impact energies.

The values of resistance and E_{sb} of specimen Adh-1 are taken as reference value to analyze and understand the effectiveness of core/facing interface performance. The percentage of increase of the resistance and E_{sb} values of other specimens are calculated and plotted in Fig. 15. It is observed that increasing the percentage (value) of the core/facing interface resistance increases effectiveness percentage. Meanwhile as the initial impact energy increases from 50 to 100 J, the E_{sb} values and effectiveness percentage also increased. As given in Fig. 15, changing the initial impact energy from 50 to

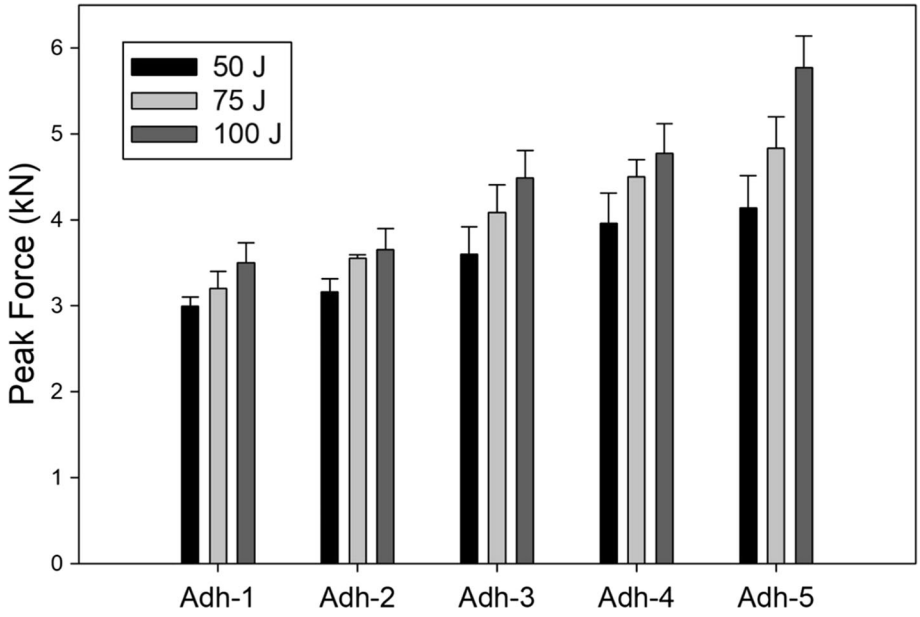

Fig. 9 The average peak load obtained for each specimen in three different initial impact energies with error bars

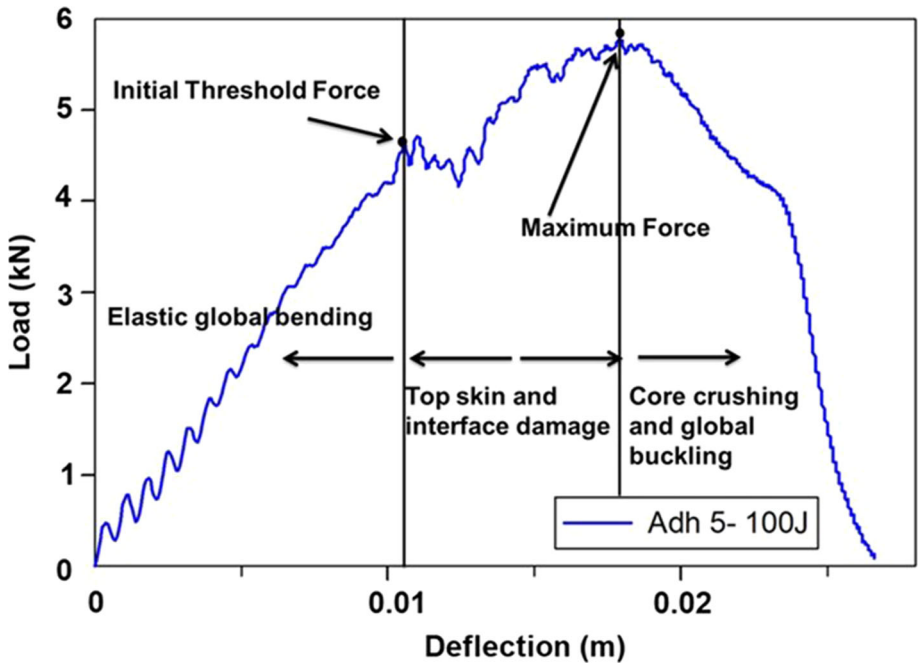

Fig. 10 A typical curve of the failure for specimen Adh-5 with 100 J impact energy

100 J produced more than 120% increase in the effectiveness of the sandwich panels in terms of energy absorbed in shear and bending deformations. The dynamic response of polymeric material is highly affected by the loading rate (Ref 47), whereas the dynamic behavior of aluminum is not so sensitive to loading rate. So, it can be concluded that total increment on the bending and shear energy absorption is due to the core/facing interface bonding material. In Fig. 12, 13, and 14, the curves of three energy levels are nonlinear with respect to the interface resistance values. It may be caused by nonlinear nature of core/face interface polymeric material. On the other hand, the total energy is shared between bending and shear stresses by increasing the interface resistance.

4. Conclusion

This study is focused on analyzing the effect of core/facing interface performance on the impact response of the aluminum honeycomb sandwich panels. The panels are fabricated using five different adhesives resulting in panels with five different core/facing interface resistance, and they are subjected to low-velocity impact loading under three different impact energy levels. Special impact force sensor and data acquisition system are used to measure the load–time histories. Newton's second law of motion and numerical integration methods are employed to obtain the load–deflection histories. In addition, the param-

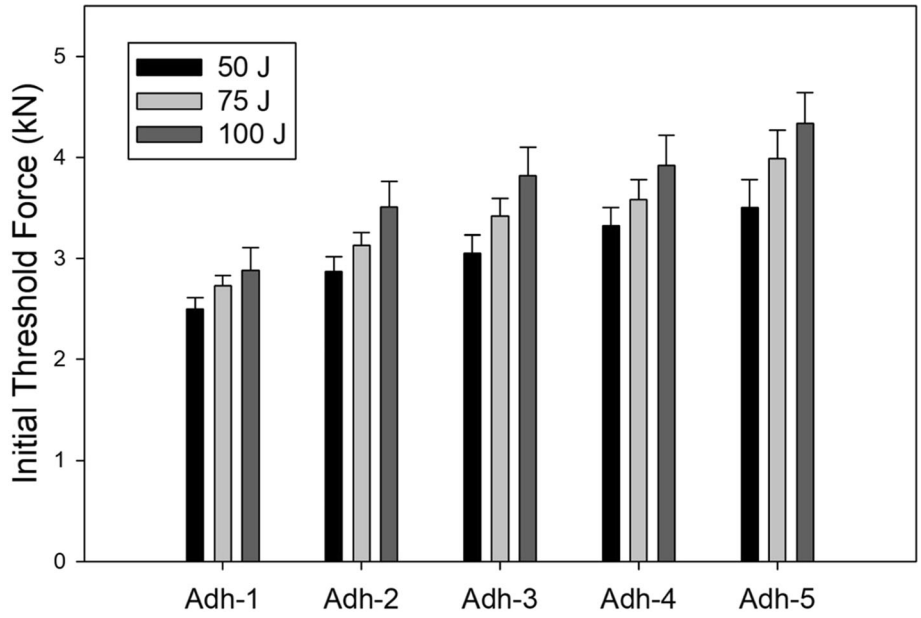

Fig. 11 Average initial threshold forces with error bars

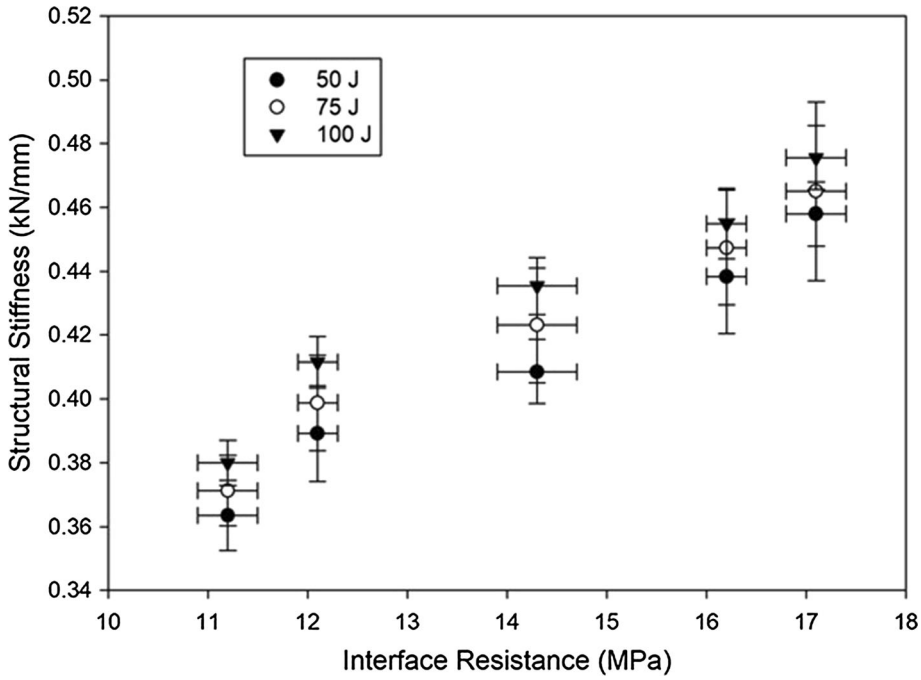

Fig. 12 Structural stiffness with respect to the adhesive interface resistance

eters or factors such as failure mechanism, the initial threshold force, peak load, maximum deflection, structural stiffness, and energy absorption are considered to assess the effect of interface resistance on the low-velocity impact response of the panels.

The experimental results show that the interface resistance is highly related to the failure mechanism. The impact damage performance of the sandwich panels is improved by using high resistance interface bonding. Debonding at the core/facing interface has occurred in specimens where the interface resistance is lower than 14.3 MPa. However, as the interface resistance is increased, the debonding area in sandwich panel is decreased. When the initial impact energy is increased, the debonding occurs in large area of core/skin interface. But in specimens with interface resistance of 16.2 MPa, debonding failure is not observed. The microstructural analysis and the morphology of core/face sheet interface of the aluminum honeycomb sandwich panels show that more voids, interface, and cohesive cracks formed in specimens with low interface resistance. When the interface resistance is increased, there is a reduction in the formation of voids, interface, and cohesive cracks. It can be concluded that the presence of these types of defects plays an important role in the impact failure of

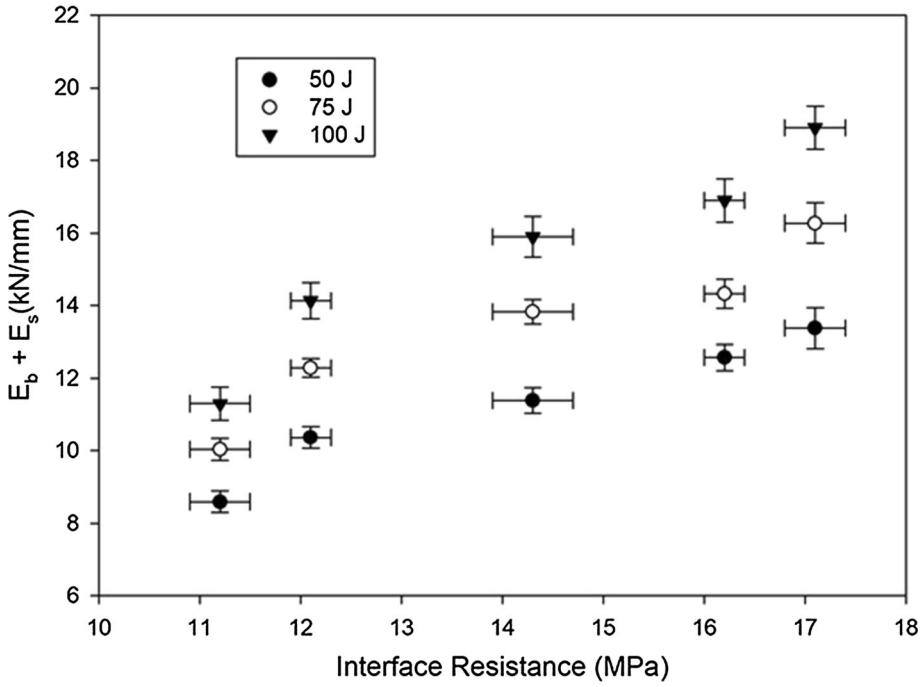

Fig. 13 The absorbed energy in bending and shear deflections with respect to the interface resistance

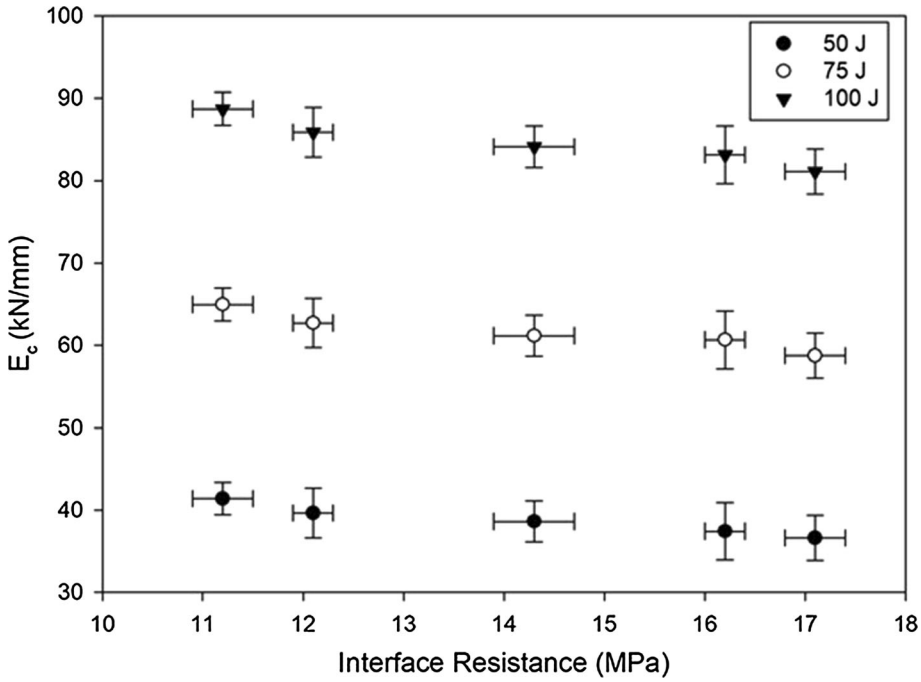

Fig. 14 The total energy absorbed in contact area with respect to the interface resistance

aluminum sandwich structures, which occurs due to large deflection of panel sheets.

The peak force of sandwich panels with 17.1 MPa interface resistance is 50% higher than the specimens with 11.2 MPa interface resistance. Meanwhile, it is observed that when there is an increase in the impact velocity, the effectiveness of interface resistance on the peak force increases. In addition, less deflection and short contact duration are observed in the sandwich panels with high interface resistance in comparison with specimens with low interface resistance.

When the initial impact velocity is increased, the panels with high interface resistance absorb more energy compared to low resistance panels. The damage mechanism and theoretical energy balance modeling are used to analyze the effectiveness of core/facing interface performance on the impact behavior of the panels. Energy balance modeling demonstrated that the energy absorbed in the bending and shear deflections increases with the increase in resistance at the core/facing interface. Changing the initial impact energy from 50 to 100 J produced more than 120% increase in the performance of the sandwich

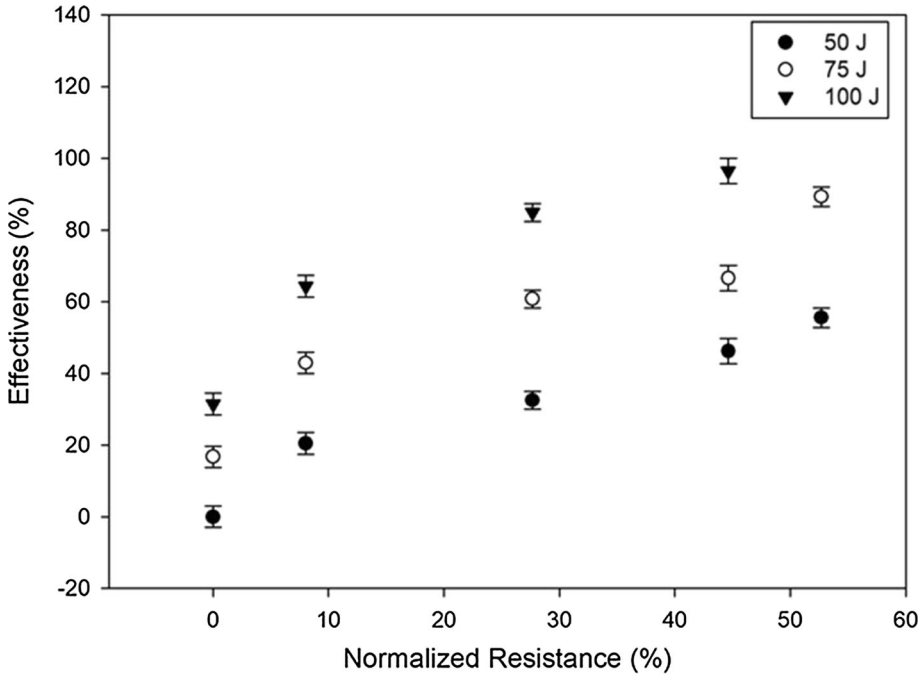

Fig. 15 The effectiveness of core/facing interface resistance in relation to the normalized resistance

panels in terms of energy absorbed in shear and bending deformations.

Acknowledgments

The authors would like to thank Altıgen Space Aviation Ship Construction Inc., Konya, Turkey, for their support in kindly supplying the honeycomb sandwich panels. Also, the authors would like to thank Enago (www.enago.com) for the English language review. The authors are grateful to Professor Mesut Uyaner for sharing his laboratory facilities.

References

1. B.M.B. Mertani, B. Keskes, and M. Tarfaoui, Experimental Analysis of the Crushing of Honeycomb Cores Under Compression, *J. Mater. Eng. Perform.*, 2019, **28**(3), p 1628–1638
2. L. Cai, D. Zhang, S. Zhou, and W. Xu, Investigation on Mechanical Properties and Equivalent Model of Aluminum Honeycomb Sandwich Panels, *J. Mater. Eng. Perform.*, 2018, **27**(12), p 6585–6596
3. A.J. Turner, M. Al Rifaie, A. Mian, and R. Srinivasan, Low-Velocity Impact Behavior of Sandwich Structures with Additively Manufactured Polymer Lattice Cores, *J. Mater. Eng. Perform.*, 2018, **27**(5), p 2505–2512
4. A.P. Meran, T. Toprak, and A. Muğan, Numerical and Experimental Study of Crashworthiness Parameters of Honeycomb Structures, *Thin Wall Struct.*, 2014, **78**, p 87–94
5. L. Pehlivan and C. Baykasoğlu, An Experimental Study on the Compressive Response of CFRP Honeycombs with Various Cell Configurations, *Compos. B Eng.*, 2019, **162**, p 653–661
6. A.P. Meran and A. Samanci, Analysis of Various Composite Patches Effect on Mechanical Properties of Notched Al-Mg Plate, *Steel Compos. Struct.*, 2017, **25**(6), p 685–692
7. A.P. Meran, C. Baykasoğlu, A. Muğan, and T. Toprak, Development of a Design for a Crash Energy Management System for Use in a Railway Passenger Car, *Proc. Inst. Mech. Eng. F J. Rail Rapid Transit*, 2016, **2301**, p 206–219
8. M.H. Fatt and K.S. Park, Perforation of Honeycomb Sandwich Plates by Projectiles, *Compos. A Appl. Sci.*, 2000, **318**, p 889–899
9. J. Wang, A.M. Waas, and H. Wang, Experimental and Numerical Study on the Low-Velocity Impact Behavior of Foam-Core Sandwich Panels, *Compos. Struct.*, 2013, **96**, p 298–311
10. S. Zhu and G.B. Chai, Low-Velocity Impact Response of Composite Sandwich Panels, *Proc. Inst. Mech. Eng. F J. Rail Rapid Transit*, 2016, **2302**, p 388–399
11. C. Menna, A. Zinno, D. Asprone, and A. Prota, Numerical Assessment of the Impact Behavior of Honeycomb Sandwich Structures, *Compos. Struct.*, 2013, **106**, p 326–339
12. A. Akatay, M.Ö. Bora, O. Çoban, S. Fidan, and V. Tuna, The Influence of Low Velocity Repeated Impacts on Residual Compressive Properties of Honeycomb Sandwich Structures, *Compos. Struct.*, 2015, **125**, p 425–433
13. Y. Chen, S. Hou, K. Fu, X. Han, and L. Ye, Low-Velocity Impact Response of Composite Sandwich Structures: Modelling and Experiment, *Compos. Struct.*, 2017, **168**, p 322–334
14. J. Wang, J. Li, and H. Ganga-Rao, Low-Velocity Impact Responses and CAI, Properties of Synthetic Foam Sandwiches, *Compos. Struct.*, 2019, **220**, p 412–422
15. R. Gunes and K. Arslan, Development of Numerical Realistic Model for Predicting Low-Velocity Impact Response of Aluminium Honeycomb Sandwich Structures, *J. Sandwich Struct. Mater.*, 2016, **18**(1), p 95–112
16. C.C. Foo, L.K. Seah, and G.B. Chai, Low-Velocity Impact Failure of Aluminium Honeycomb Sandwich Panels, *Compos. Struct.*, 2008, **851**, p 20–28
17. D. Zhang, Q. Fei, and P. Zhang, Drop-Weight Impact Behavior of Honeycomb Sandwich Panels Under a Spherical Impactor, *Compos. Struct.*, 2017, **168**, p 633–645
18. T. Anderson and E. Madenci, Experimental Investigation of Low-Velocity Impact Characteristics of Sandwich Composites, *Compos. Struct.*, 2000, **503**, p 239–247
19. M.V. Hosur, M. Abdullah, and S. Jeelani, Manufacturing and Low-Velocity Impact Characterization of Foam Filled 3-D Integrated Core Sandwich Composites with Hybrid Face Sheets, *Compos. Struct.*, 2005, **692**, p 167–181
20. M.A. Bhuiyan, M.V. Hosur, and S. Jeelani, Low-Velocity Impact Response of Sandwich Composites with Nanophased Foam Core and Biaxial ± 45 Braided Face Sheets, *Compos. B Eng.*, 2009, **406**, p 561–571

21. H. Wang, K.R. Ramakrishnan, and K. Shankar, Experimental Study of the Medium Velocity Impact Response of Sandwich Panels with Different Cores, *Mater. Des.*, 2016, **9**, p 68–82
22. A. Dogan and V. Arikan, Low-Velocity Impact Response of E-Glass Reinforced Thermoset and Thermoplastic Based Sandwich Composites, *Compos. B Eng.*, 2017, **127**, p 63–69
23. E.J. Herup and A.N. Palazotto, Low-Velocity Impact Damage Initiation in Graphite/Epoxy/Nomex Honeycomb-Sandwich Plates, *Compos. Sci. Technol.*, 1998, **5712**, p 1581–1598
24. G. Petrone, S. Rao, S. De Rosa, B.R. Mace, F. Franco, and D. Bhattacharyya, Behaviour of Fibre-Reinforced Honeycomb Core Under Low Velocity Impact Loading, *Compos. Struct.*, 2013, **100**, p 356–362
25. Y. Wu, Q. Liu, J. Fu, Q. Li, and D. Hui, Dynamic Crash Responses of Bio-inspired Aluminum Honeycomb Sandwich Structures with CFRP Panels, *Compos. B Eng.*, 2017, **121**, p 122–133
26. M.R. Yellur, H. Seidlitz, F. Kuke, K. Wartig, and N. Tsombanis, Low Velocity Impact Study on Press Formed Thermoplastic Honeycomb Sandwich Panels, *Compos. Struct.*, 2019, **225**, p 111061
27. J. Liu, W. He, D. Xie, and B. Tao, The Effect of Impactor Shape on the Low-Velocity Impact Behavior of Hybrid Corrugated Core Sandwich Structures, *Compos. B Eng.*, 2017, **111**, p 315–331
28. G. Sun, D. Chen, H. Wang, P.J. Hazell, and Q. Li, High-Velocity Impact Behaviour of Aluminium Honeycomb Sandwich Panels with Different Structural Configurations, *Int. J. Impact Eng.*, 2018, **122**, p 119–136
29. Y.O. Shen, F.J. Yang, W.J. Cantwell, S. Balawi, and Y. Li, Geometrical Effects in the Impact Response of the Aluminium Honeycomb Sandwich Structures, *J. Reinf. Plast. Compos.*, 2014, **3312**, p 1148–1157
30. S. Hou, C. Shu, S. Zhao, T. Liu, X. Han, and Q. Li, Experimental and Numerical Studies on Multi-layered Corrugated Sandwich Panels Under Crushing Loading, *Compos. Struct.*, 2015, **126**, p 371–385
31. W. He, L. Yao, X. Meng, G. Sun, D. Xie, and J. Liu, Effect of Structural Parameters on Low-Velocity Impact Behavior of Aluminum Honeycomb Sandwich Structures with CFRP Face Sheets, *Thin Wall Struct.*, 2019, **137**, p 411–432
32. O. Ozdemir, R. Karakuzu, and A.K.J. Al-Shamary, Core-Thickness Effect on the Impact Response of Sandwich Composites with Poly Vinyl Chloride and Poly Ethylene Terephthalate Foam Cores, *J. Compos. Mater.*, 2015, **4911**, p 1315–1329
33. M.Z. Mahmoudabadi and M. Sadighi, A Study on the Static and Dynamic Loading of the Foam Filled Metal Hexagonal Honeycomb–Theoretical and Experimental, *Mater. Sci. Eng. A Struct.*, 2011, **530**, p 333–343
34. V. Crupi, G. Epasto, and E. Guglielmino, Collapse Modes in Aluminium Honeycomb Sandwich Panels Under Bending and Impact Loading, *Int. J. Impact Eng.*, 2012, **43**, p 6–15
35. S. Zhu and G.B. Chai, Damage and Failure Mode Maps of Composite Sandwich Panel Subjected to Quasi-Static Indentation and Low Velocity Impact, *Compos. Struct.*, 2013, **101**, p 204–214
36. H. Ebrahimi, R. Ghosh, E. Mahdi, H. Nayeb-Hashemi, and A. Vaziri, Honeycomb Sandwich Panels Subjected to Combined Shock and Projectile Impact, *Int. J. Impact Eng.*, 2016, **95**, p 1–11
37. W. Huang, W. Zhang, D. Li, N. Ye, W. Xie, and P. Ren, Dynamic Failure of Honeycomb-Core Sandwich Structures Subjected to Underwater Impulsive Loads, *Eur. J. Mech. A Solid*, 2016, **60**, p 39–51
38. W.S. Burton and A.K. Noor, Structural Analysis of the Adhesive Bond in a Honeycomb Core Sandwich Panel, *Finite Elem. Anal. Des.*, 1997, **263**, p 213–227
39. A.B. Pereira and F.A. Fernandes, Sandwich Panels Bond with Advanced Adhesive Films, *J. Compos. Sci.*, 2019, **3**(3), p 79
40. S. Zhu and G.B. Chai, Effect of Adhesive in Sandwich Panels Subjected to Low-Velocity, *Proc. Inst. Mech. Eng. L J. Mater. Des. Appl.*, 2011, **2253**, p 171–181
41. D. Zhang, D. Jiang, Q. Fei, and S. Wu, Experimental and Numerical Investigation on Indentation and Energy Absorption of a Honeycomb Sandwich Panel Under Low-Velocity Impact, *Finite Elem. Anal. Des.*, 2016, **117**, p 21–30
42. M.Z. Mahmoudabadi and M. Sadighi, Experimental Investigation on the Energy Absorption Characteristics of Honeycomb Sandwich Panels Under Quasi-Static Punch Loading, *Aerosp. Sci. Technol.*, 2019, **88**, p 273–286
43. X. Liu, G. Du, H. Yan, and S. Cheng, *Failure Analysis of Adhesive Surface Damage in Sandwich Plates Under Compressed Loads*, Adv. Mater. Struct., Mech, 2019, https://doi.org/10.1080/15376494.2019.1567883
44. I.M. Daniel, E.E. Gdoutos, K.A. Wang, and J.L. Abot, Failure Modes of Composite Sandwich Beams, *Int. J. Damage Mech.*, 2002, **114**, p 309–334
45. C.C. Foo, G.B. Chai, and L.K. Seah, A Model to Predict Low-Velocity Impact Response and Damage in Sandwich Composites, *Compos. Sci. Technol.*, 2008, **68**, p 1348–1356
46. M.A. Hazizan and W.J. Cantwell, The Low Velocity Impact Response of Foam-Based Sandwich Structures, *Compos. B Eng.*, 2002, **33**, p 193–204
47. A. Meram, Dynamic Characterization of Elastomer Buffer Under Impact Loading by Low-Velocity Drop Test Method, *Polym. Test.*, 2019, **79**, p 106013